



LJMU Research Online

AL-Ansari, NA, Abdellatif, M, Ezeelden, M, Ali, SS and Knutsson, S

Climate Change and Future Long Term Trends of Rainfall at North-eastern Part of Iraq

<http://researchonline.ljmu.ac.uk/id/eprint/2346/>

Article

Citation (please note it is advisable to refer to the publisher's version if you intend to cite from this work)

AL-Ansari, NA, Abdellatif, M, Ezeelden, M, Ali, SS and Knutsson, S (2014) Climate Change and Future Long Term Trends of Rainfall at North-eastern Part of Iraq. Journal of Civil Engineering and Architecture, 8 (6). pp. 790-805. ISSN 1934-7367

LJMU has developed **LJMU Research Online** for users to access the research output of the University more effectively. Copyright © and Moral Rights for the papers on this site are retained by the individual authors and/or other copyright owners. Users may download and/or print one copy of any article(s) in LJMU Research Online to facilitate their private study or for non-commercial research. You may not engage in further distribution of the material or use it for any profit-making activities or any commercial gain.

The version presented here may differ from the published version or from the version of the record. Please see the repository URL above for details on accessing the published version and note that access may require a subscription.

For more information please contact researchonline@ljmu.ac.uk

<http://researchonline.ljmu.ac.uk/>

Climate Change and Future Long Term Trends of Rainfall at North-eastern Part of Iraq

Nadhir Al-Ansari¹, Mawada Abdellatif², Mohammad Ezeelden³, Salahalddin S. Ali⁴, Sven Knutsson⁵

^{1,5}Lulea University, Sweden, ²Liverpool JM University, UK, ³Mosul University, Iraq, ⁴Sulaimani University, Iraq

Correspondence to: N. A. Al-Ansari (nadhir.alansari@ltu.se)

Abstract

Iraq is facing water shortage problem despite the presence of the Tigris and Euphrates Rivers. In this research, long rainfall trends up to the year 2099 were studied in Sulaimani city northeast Iraq to give an idea about future prospects. Two emission scenarios used by the Intergovernmental Panel on Climate Change (A2 & B2) were employed. The results indicates that the average annual rainfall show a significant downward trend for both A2 and B2 scenarios. In addition, winter projects some increase/decrease in the daily rainfall statistics of wet days, the spring season show very slight drop and no change for both scenarios. However both summer and autumn show a significant reduction in maximum rainfall value especially in 2080s while the other statistics remain nearly the same.

The extremes events are to decrease slightly in 2080s with highest decrease associated with A2 scenario. This because the rainfall under scenario A2 is more significant than under scenario B2 and temperature can be very hot and worse with increase in emission scenario which causes the moist air to be evaporated before going up and cause the rainfall. The return period of a certain rainfall will increase in the future when a present storm of 20 year could occur once every 43 year in the 2080s. An increase in the frequency of extreme rainfall depends on the return period, season of the year, the future period considered and the emission scenario under which it will occur.

Keywords: Iraq, Rainfall, Climate change, Sulaimani

1 Introduction

The Middle East and North Africa (MENA region) is considered as an arid to semi-arid region where annual rainfall is about 166mm [1]. Water resources in this region are scarce and the region is threatened by desertification. Climate change; population growth and development are other factors creating another burden on the water resources of the region. Salem [2] stated that 90% of the available water resources will be consumed in 2025.

UN considers nations having less than 1500, 1000 and 500 cubic meters per capita per year as under water stress, under water scarcity severe water stress respectively. The average annual available water per capita in MENA region was 977 cubic meters in 2001 and it will decrease to 460 cubic meters in 2023 [3,4]. For this reason, the scarcity of water resources in the MENA region, and particularly in the Middle East, represents an extremely important factor in the stability of the region and an integral element in its economic development and prosperity [5,6].

The situation will be more severe in future [7,8]. Climate change is one of the main factors for future shortages expected in the region [9]. At the end of the century the mean temperatures in the MENA region are projected to increase by 3°C to 5°C while the precipitation will decrease by about 20% [10]. According to IP CC [11] water run-off will be reduced by 20% to 30% in most of MENA by 2050 and water supply might be reduced by 10% or greater by 2050 [12].

Iraq was considered rich in its water resources due to the presence of the Tigris and Euphrates Rivers. A major decrease in the flow of the rivers was experienced when Syria and Turkey started to build dams on the upper parts of these rivers [13]. Tigris and Euphrates discharges will continue to decrease with time and they will be completely dry up by 2040 [14]. In addition, future rainfall forecast showed that it is decreasing in Iraq's neighbouring "Jordan" [15,16,17].

In this research, rainfall records dated back to 1940 for Sulaimani city were studied and used in this research. These data were used in two different models to evaluate long term rainfall amounts expected in northeast Iraq due to two scenarios of climate change. This will help farmers and decision makers to take precautions to overcome water shortages.

2 Studied area

Iraq occupies a total area of 437 072 square kilometres. Land forms 432 162 square kilometres while water forms 4910 square kilometres of the total area. Iraq is bordered by Turkey from the north, 352km, Iran from the east, 1458 km, Syria and Syria from the west, 605 km and 181 km, respectively and Saudi Arabia and Kuwait from the south, 814 km and 240 km, respectively (Fig. 1). The total population in Iraq is about 30,000,000. Iraq is composed of 18 Governorates (Fig. 1). Topographically, Iraq is divided into 4 regions (Fig. 2). The mountain region occupies 5% of the total area of Iraq, restricted at the north and north eastern part of the country. This region is part of Taurus -Zagrus mountain range. Plateau and Hills Regions is the second region and it represents 15% of the total area of Iraq. This region is bordered by the mountainous region at the north and the Mesopotamian plain from the south. The Mesopotamian plain is the third region and it is restricted between the main two Rivers, Tigris and Euphrates. It occupies 20% of the total area of Iraq. This plain extends from north at Samara, on the Tigris, to Hit, on the Euphrates, toward the Gulf in the south. The remainder area of Iraq which forms 60% of the total area is referred to as the Jazera and Western Plateau.

Sulaimaniyah Governorate is located northeast Iraq on the border with Iran within the mountain region (Fig. 2). The area of the governorates reaches 17023 square kilometres which forms 9.3% of the total area of Iraq. The population of the governorate reaches 1878800, and in the capital city of the governorate reaches 725000. The area is characterized by its mountains. The maximum elevation reaches maximum altitude of 3500 meter above sea level in the northeast while it drops to 400 m a.s.l in the southern part.



Fig. 1. Physiography of Iraq

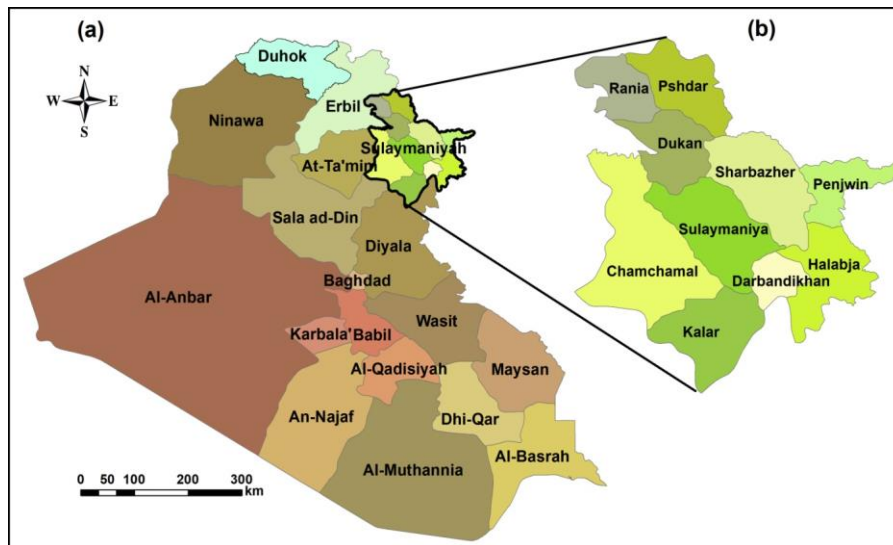


Fig. 2. Map of Iraq with enlarge view of the ten districts of Sulaimani (Sulaimaniyah) Governorate.

The weather in the summer is rather warm, with temperatures ranging from 15°C to 40°C and sometimes up to 45°C. The city is usually windy during winter and there are spills of snow

falling sometimes. This season extends from December till February. However, the temperature in the winter season is about 7.6°C. The average relative humidity for summer and winter are 25.5% and 65.6% respectively, while the evaporation reached 329.5 mm in summer and 53 mm in Winter where the average wind speed in winter 1.2 m. sec⁻¹ and little bit more in summer 1.8 m. sec⁻¹. Sunshine duration for winter is half its values for summer where it reaches 5.1 and 10.6 hr in winter and summer respectively. Average monthly rainfall in winter reaches 110.1 mm. Rainfall season starts in October at Sulaimani with light rainfall storms and it intensifies during November and continues till May.

3 Data extraction

The daily atmospheric variables were derived from the National Centre for Environmental Prediction (NCEP/NCAR) (NCEP) reanalysis data set [18] for a period of January 1980 to December 2001. The data have a horizontal resolution of 2.5° lat. by 2.5° long. The daily rainfall data was obtained from Iraqi Meteorological Office and available for the period January 1980 to December 2001. The met office in UK provides GCM data for a number of surface and atmospheric variables for the HadCM3 Global Climate Model (third version) which has a horizontal resolution of roughly 2.5° latitude by 3.75° longitude and a vertical resolution of 29 levels. These data has been used in the present study and comprise of present-day and future simulations forced by two emission scenarios, namely A2 and B2. The medium high (A2) and medium low B2 scenarios have been used for purpose of this study as they are more likely than others scenarios, that beside the fact that no climate modelling centre has performed GCM simulations for more than a few emissions scenarios (HadCM3 has only these two scenarios) otherwise pattern scaling can be used for generating different scenarios which entail a huge uncertainty. The GCM data is re-gridded to a common 2.5° using inverse square interpolation technique [19]. The utility of this interpolation algorithm was examined in previous down-scaling studies [20,21].

4 Methodology

General circulation models (GCMs) solve the principal physics equations of the dynamics of the atmosphere and of the oceans together with their interactions on a 3-D grid over the globe. GCMs allow us to simulate climate variables and to study the mechanisms of the

present, past, and future climate of the Earth. However due to the coarse scale of the GCM in order of hundred kilometres, downscaling approach is generally used to obtain local scale feature. Overview of downscaling approaches has been provided elsewhere (see [22,23]).

In line with the scope of this study that simple approaches across a wide range of application are preferable. The present study used statistical downscaling (SD) method that is considered as one of the most cost-effective methods in local-impact assessments of climate scenarios and weather forecast. The statistical downscaling (SD) is cheap to run and universally applicable, this is why the current study has been applied it to the case study of Iraq.

4.1 Optimization of Predictors

Determination of appropriate predictors for the input layer is very important to build the downscaling of rainfall model. This process tends not only to drop out those variables that have less influence on the output to avoid over fitting but also to overcome the shortage of historical record used for calibration processes. This study takes into account the physically based consideration regarding the rainfall evolution. As addressed in the previous section, the study area is dominated by the orographic rainfall, therefore, among the range of variables provided by the NCEP/NCAR data, only few variables which are driving factors for the orographic rainfall evolution were selected in the calibration processes. So Predictors screening was conducted to finalize a good set of predictors based on “stepwise regression” or known as forward regression. It yields the most powerful and parsimonious model as has been shown by previous studies [24,25].

4.2 Developing Downscaling Rainfall Model

Artificial neural network is simply understood as a nonlinear statistical data modelling tool that presents complex relationships between predictors (input layer) and predictants (output layer) through a synapse system hidden layers connecting predictors with predictants, or the so called required outputs . As a result, ANN has demonstrated its wide range of application to solve complicated problems in many fields, for instance, engineering and environment [26].

For the current application of ANN as downscaling technique, ANN aims at directly translating large-scale data into local-scale values by performing nonlinear regressions. The large scale observed NCEP climatic variable and local scale observed rainfall were used to

build this relationship. Then large scale predictors from GCM were fed into the ANN model to generate local scale future projection. In SD approach, it is assumed that this relation is constant with changing climate. Each set of selected predictor variables in the previous section were used to calibrate and validate the corresponding dynamic neural networks downscaling method for four seasons winter (JFD), spring (MAM), summer (JJA) and autumn (SON). Figure 3 show the structure of ANN used in building rainfall downscale model with k neurons for the hidden layer 1 and J neurons for hidden layer 2 and w weights of the link that connected all ANN layers.

Since GCMs do not always perform well at simulating the climate of a particular region this means that there may be large differences between observed and GCM-simulated conditions (i.e., GCM bias or error). This could potentially violate the statistical assumptions associated with SD and give poor results if the predictor data were not normalised [27]. The normalisation process ensures that the distributions of observed and GCM-derived predictors are in closer agreement than those of the raw observed and raw GCM data. So all the inputs of the ANN model have been normalised as show in Figure 3.

All of the ANN models developed herein contain a mapping ANN architecture and are based on supervised learning. In the developed network, the learning method used is a feed forward back propagation, and the sigmoid and linear functions are the transfer function used in the hidden and output layer respectively. The three-layer network with two hidden layers was selected as the best configuration. The number of nodes in each layer differs according to the selected model (see results below). These node numbers were determined after a systematic study of each model. There are different backpropagation algorithms, however in the present application, Levenberg-Marquardt approach (LM) [28,29] has been applied. It is usually 10 to 100 times faster, stable and more reliable than any other back-propagation techniques. The main objective behind all ANN training algorithm is to minimise a certain error function E. The quantity E, usually the Mean Square Error, measures the difference between the observed (o) and Target (d) values for a data with size (n) [30],

$$E = \frac{1}{p} \left(\sum_i^n (o(i) - d(i))^2 \right) \dots\dots\dots (1)$$

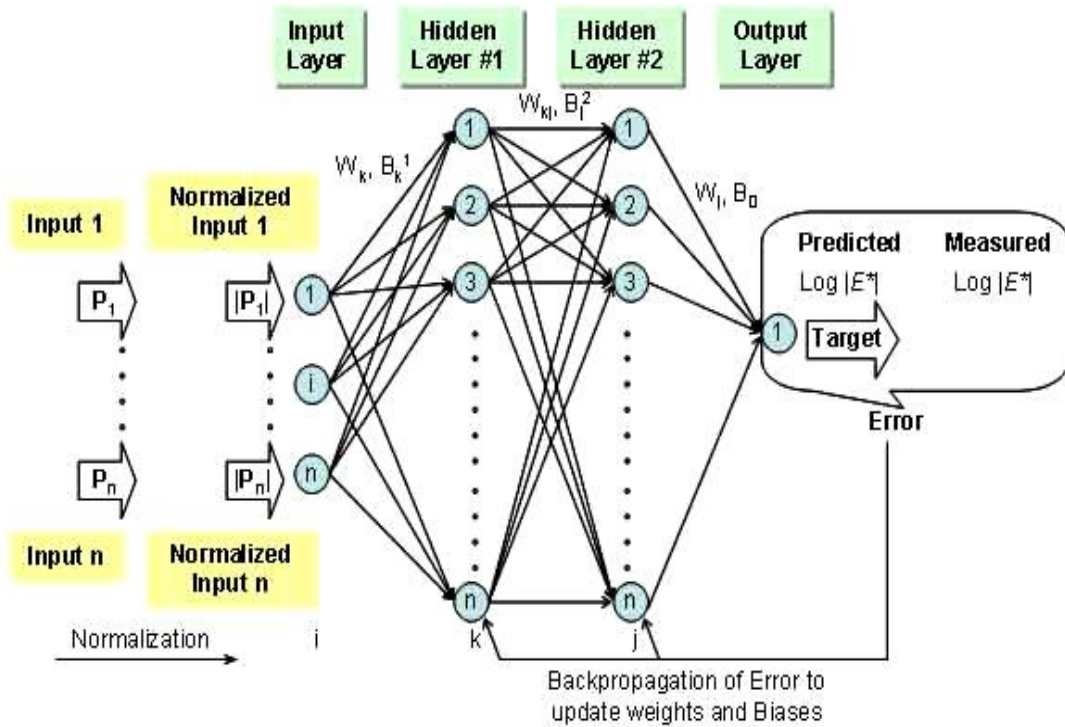


Fig. 3. Network structure used for training the ANN models

5 Results and discussion

Downscaling models for the four seasons winter, spring, summer and autumn were developed following the methodology as discussed in preceding section. The results and discussion are presented in this section.

5.1 Potential Predictors

Before building the ANN regression model for rainfall, it is important to screen the suitable climatic variables which influence the rainfall feature in the studied region and hence form predictor-predict and relationship. Table 1 displays the main predictors in the seasonal rainfall models of winter; spring, summer and autumn. The addition of each new predictor to a model was tested using a stepwise procedure and assessing the partial and zero correlations, a measure of the relative goodness-of-fit based on significance.

The key variable such as meridional velocity is shown to be important predictor for all seasons in determining rainfall. Relative humidity and airflow strength at different levels (surface, 500 and 850) are shown to be important in all seasons except summer and winter respectively. Zonal velocity, at the surface or 500hPa level, would appear to be important predictor of rainfall during the autumn and summer months. While temperature and wind

direction play an important role for the autumn, spring and winter months, this effect was not found in summer although it is characterized with warm weather that could be due to inclusion of effect of altitude in the region. The effect of correlation for geopotential height at 500 and vorticity at 850 was captured in spring only. Table 1 show ranges of significant correlation between 0.013-0.136 and 0.01-0.124 for zero and partial correlation respectively with significant level of less than 5% which results in number of selected predictors ranged between 3-8 predictors across the four seasons.

5.2 Rainfall Model Feature and Efficiency

To adequately assess the ability of the ANN technique employed to capture the underlying relationships between the large-scale atmospheric predictors and rainfall, the data was split into three periods, one for calibration & validation and that applied during the training process and another set for independent verification purposes after the training terminate. The validation period is normally applied for ANN during the training to monitor the training error in order to avoid the over fitting. The calibration and validation periods for the four seasonal models were selected randomly within the period 1980–2001. Different percentages have been tested to investigate the suitable ratio which results in 80% of the data were selected for calibration, 5% for validation and 15% for verification. When calibrating the ANN, outliers were found to have a large impact on the resulting models and were excluded from subsequent analysis.

Table 1. Selected Climate variable (predictors)

| Predictors | JFD | | | MAM | | | JJA | | | SON | | |
|----------------------------------|-------|------------|---------------------|-------|------------|---------------------|-------|------------|---------------------|-------|------------|---------------------|
| | sig | Zero-order | Partial correlation |
| Zonal velocity | - | - | - | - | - | - | 0.025 | 0.05 | -0.036 | - | - | - |
| Lagged Zonal | - | - | - | - | - | - | - | - | - | 0.027 | 0.040 | 0.067 |
| Meridional velocity | - | - | - | - | - | - | - | - | - | 0.001 | -0.013 | 0.098 |
| Lagged meridional | 0.001 | 0.039 | 0.116 | - | - | - | - | - | - | - | - | - |
| Lagged meridional | - | - | - | - | - | - | 0.002 | 0.073 | 0.050 | - | - | - |
| Meridional velocity (850) | - | - | - | 0.001 | -0.056 | -0.052 | - | - | - | - | - | - |
| Airflow strength(850) | - | - | - | 0.004 | 0.029 | 0.046 | - | - | - | - | - | - |
| Lagged airflow | - | - | - | - | - | - | 0.003 | 0.068 | 0.049 | 0.004 | 0.032 | -0.010 |
| Relative humidity | 0.000 | -0.069 | -0.124 | - | - | - | - | - | - | - | - | - |
| Lagged Relative humidity | - | - | - | 0.000 | 0.116 | 0.064 | - | - | - | 0.006 | 0.154 | 0.084 |
| Relative humidity(500) | - | - | - | 0.001 | 0.044 | 0.053 | - | - | - | - | - | - |
| Lagged relative | - | - | - | - | - | - | - | - | - | .085 | .099 | 0.052 |
| Relative humidity(850) | - | - | - | 0.000 | 0.051 | -0.070 | - | - | - | - | - | - |
| Lagged relative | 0.002 | 0.063 | 0.108 | - | - | - | - | - | - | - | - | - |
| Wind direction | - | - | - | - | - | - | - | - | - | 0.004 | -0.098 | -0.088 |
| Wind direction(850) | - | - | - | - | - | - | - | - | - | 0.001 | -0.086 | -0.101 |
| Lagged wind direction | 0.000 | -0.094 | -0.102 | - | - | - | - | - | - | - | - | - |
| divergence | 0.011 | 0.010 | 0.090 | - | - | - | - | - | - | - | - | - |
| Geopotential height (500) | - | - | - | 0.012 | -0.082 | 0.041 | - | - | - | - | - | - |
| Lagged vorticity (850) | - | - | - | 0.045 | 0.025 | 0.033 | - | - | - | - | - | - |
| Temperature | - | - | - | - | - | - | - | - | - | 0.047 | -0.136 | -0.060 |
| Lagged Temperature | - | - | - | 0.000 | -0.126 | -0.058 | - | - | - | - | - | - |

Structures of the neural networks used in building the models are shown in Figure 4. It can be deduced from the network structures in Figure 4 that the ANN modelling approach employs a larger number of neurons in the hidden layers for all seasons. This larger number of neurons in the hidden layers generally contributes to the accuracy of the model.

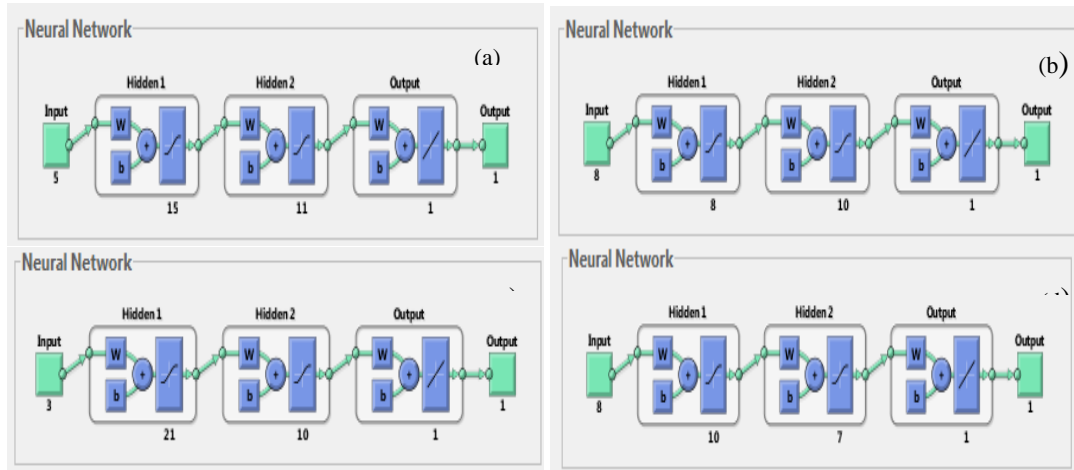


Fig. 4. Structure of ANN for (a) winter, (b) spring, (c) summer and (d) autumn

Table 2 shows results of the model produced from ANN against the observed data for each season in respect of mean, standard deviation and skewness. Generally all the fitted seasonal models perform well, as they reproduce the mean exactly. Nevertheless, looking at the model results in terms of standard deviation and skewness, there is some over/underestimation respectively across the whole seasons. This can be attributed to the fact that study area has the high rainfall variability and skewness (intense rainfall) due to the location in the mountainous area.

Table 2. Statistics of model-computed versus observed daily rainfall for years 1980–20001.

| Parameter | Mean | | Standard deviation | | skewness | |
|------------|----------|-----------|--------------------|-----------|----------|-----------|
| | Observed | Simulated | Observed | Simulated | Observed | Simulated |
| JFD | 4.01 | 4.19 | 9.71 | 7.82 | 4.69 | 6.77 |
| MAM | 2.56 | 2.54 | 7.33 | 5.45 | 5.37 | 6.83 |
| JJA | 0.01 | 0.01 | 0.16 | 0.14 | 37.57 | 38.71 |
| SON | 0.87 | 0.89 | 4.75 | 4.05 | 9.53 | 12.39 |

Figures 5 and 6 shows the comparison between monthly rainfall for both the observed and modelled series for the calibration and verification periods (1980-2001) which demonstrate a good degree of correspondence. The visual plot in Figure 4 shows the monthly average wet days for the observed and modelled rainfall for calibration and validation periods. The plot shows that the model is slightly over and under estimate the rainfall for some months by up to 2days which demonstrated that ANN is a good choice for downscaling future rainfall. This would entail the assumption that model parameters are assumed time invariant and would not change in future. So both monthly pattern (wet days and rainfall) would appear to have been adequately captured by the model, an important requirement when assessing climate impacts on such systems as the hydrological system.

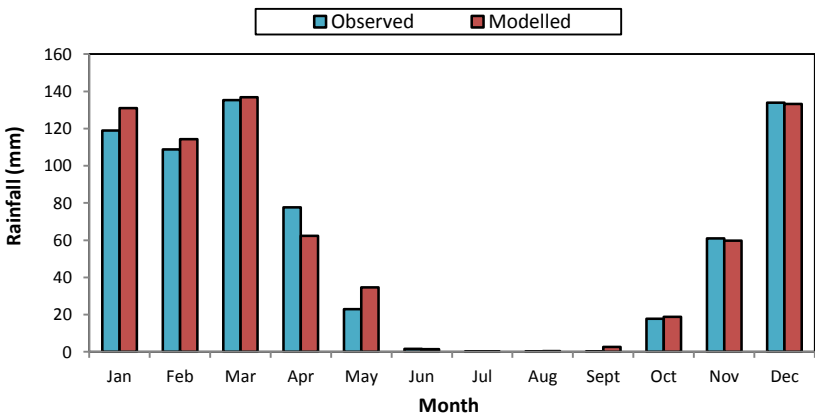


Fig. 5. Average monthly rainfall of the observed & simulated rainfall during calibration and validation periods (1980–2001).

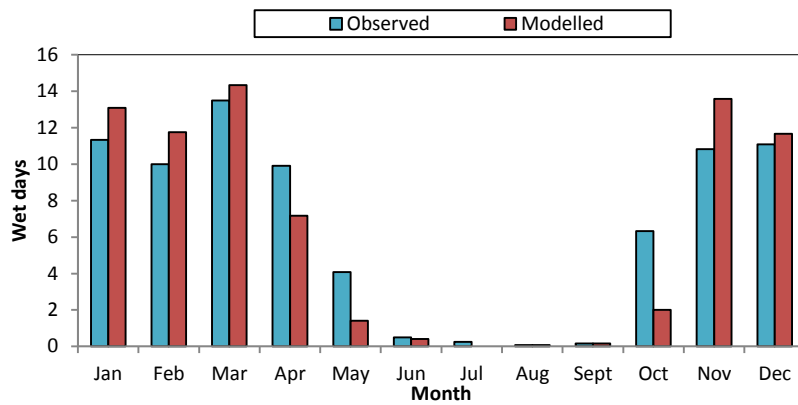
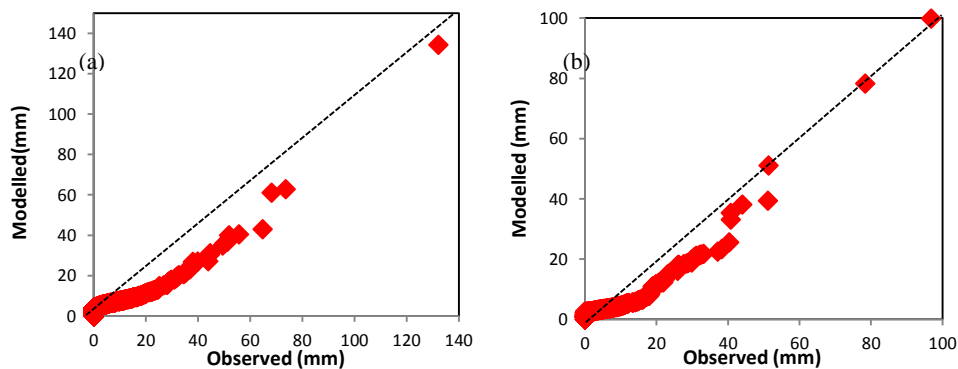


Fig. 6. Average monthly numbers of wet days of the observed & simulated rainfall during calibration and validation periods (1980–2001).

Furthermore, quantile – quantile plots of the four seasons was used to assess the model performance by comparing the simulated rainfall against the observed one after arranged in ascending order. As seen in Figure 7, model bias was found for most storm events for the four seasons. The model output- driven rainfall prediction was a bit lower than the actual observation. A reason for this discrepancy might be explained by the converse behaviour of altitudinal dependence of precipitation between actual observation and that obtained from model outputs.



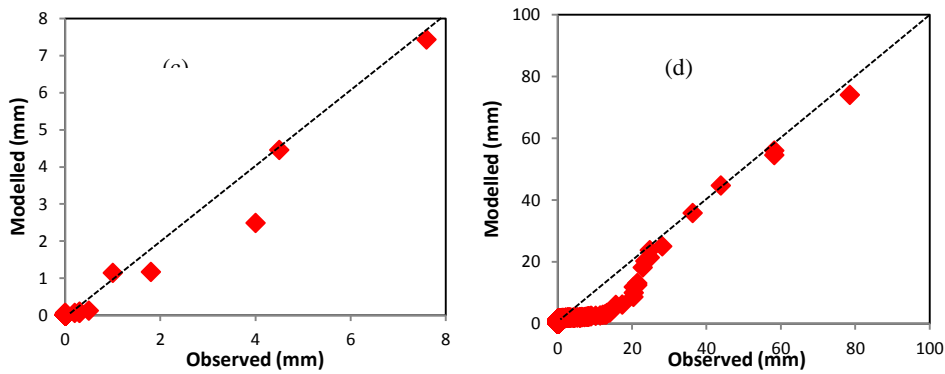


Fig. 7. Quantile – Quantile plot for observed & simulated daily rainfall for (a) winter (b) spring, (c) summer and (d) autumn during calibration and validation periods (1961-2001)

Ability of the seasonal models in reproduce the current climate were also evaluated using correlation coefficient, Nash coefficient [31], Root Mean Squared Error (RMSE) [32] and Bias [33] as in Figures 8 and 9. The autumn and summer months appear to produce the best results as represented with high the correlation and Nash coefficient of 0.88 & 0.89 and 0.77% & 0.79 respectively. As results the bias and RMSE were quite low in order of 3% and 2% as a maximum. However, all results are comparable between seasons and the correlation between day to day variability does not go below 0.60 with corresponding efficiency of 0.42, Bias 4.6% and RMSE 7.5% as a minimum and that was associated with the winter season.

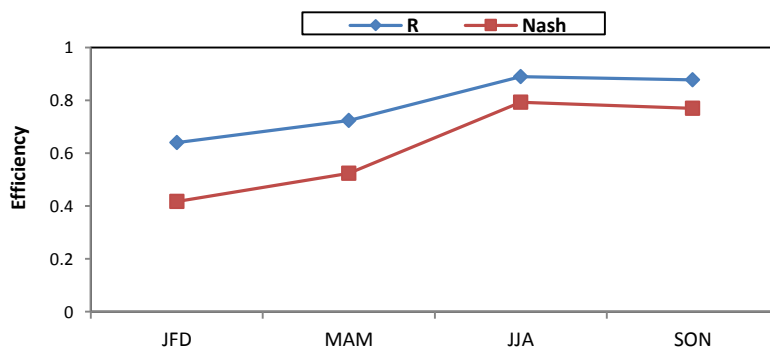


Fig. 8. ANN model efficiency in terms of correlation coefficient (R) and Nash coefficient (Nash) during calibration and validation periods (1961-2001)

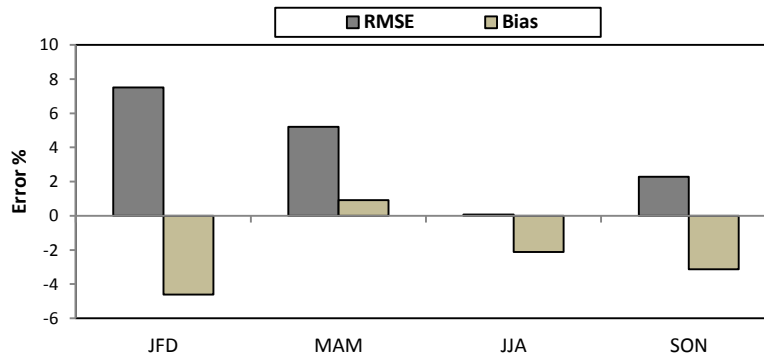


Fig. 9. ANN model error in terms of root mean square error (RMSE) and bias (Nash) during calibration and validation periods (1961-2001)

Extreme rainfall is considered one of the most important parameters used in the design of many hydrological systems. So the ability of the ANN model to reproduce extreme values of rainfall has also been assessed in this study using a combined approach of annual maximum and Generalised Extreme Value Distribution, GEV [34]. Figure 10 shows an example of the cumulative distribution function for the observed and simulated extremes (daily) rainfall at Iraq in the winter, spring, summer and autumn seasons. It can be observed in these Figures that the cumulative distribution function produced by the ANN model closely matches or exceeds the corresponding observed one for extreme rainfall at daily scale at all seasons. The conclusion that can be made from cumulative distribution function plots is that the ANN model is reasonable in representing extreme rainfall observations and their probability.

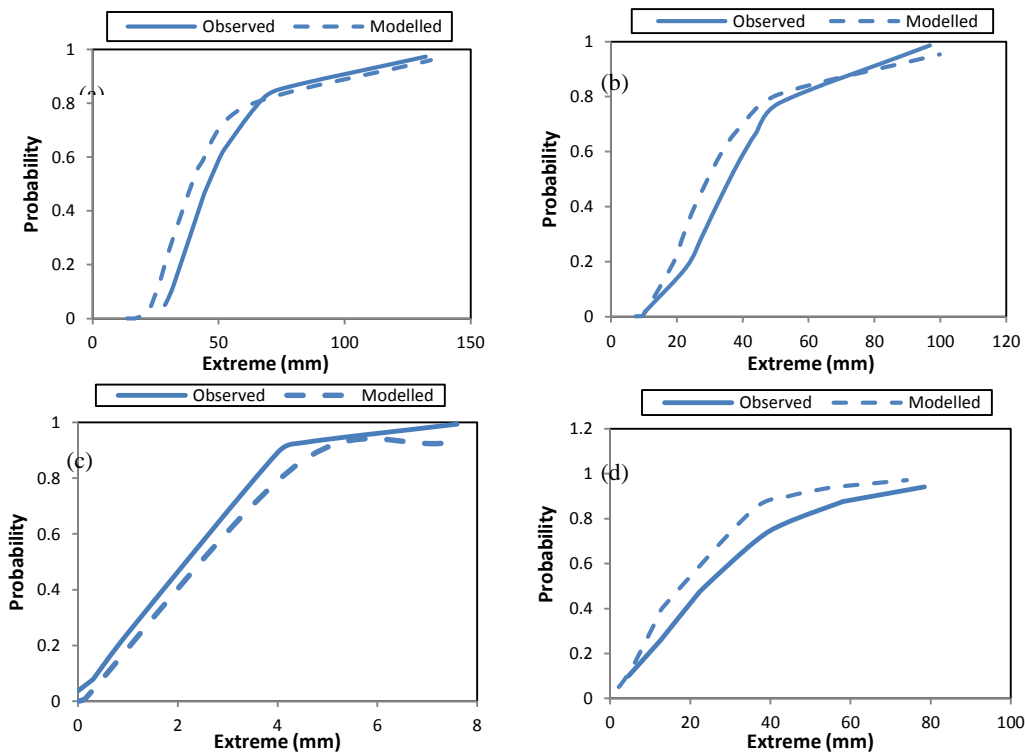


Fig. 10. CDFs of model-computed versus observed daily extremes rainfall for (a) JFD, (b) MAM, (c) JJA and (d) SON for years 1980–2001

5.3 Scenarios of Future Rainfall Projection up to 21st Century

Once the downscaling models have been calibrated and validated, the next step is to use these models to downscale the control scenario and future scenario simulated by the GCM (HadCM3). Synthetic daily rainfall time series were produced for HadCM3 A2 for a period of 139 years (1961 to 2099). The outcome was averaged and divided by three (3) period of time, which are 2020s (2010-2039), 2050s (2040-2069) and 2080s (2070-2099). Climate change was assessed by comparing these three future time slices with baseline period of 1961-1990 as recommended by the Intergovernmental Panel of Climate change.

Trend study for observed rainfall data is widely used as a base reference or a caveat of climate change studies (e.g. [35]). Also, it can provide a quick visual check for the presence of unreasonable values (outliers). However, the usefulness of trend study is always being questioned. Possible trends in the data are investigated to offer an historical context before further climate change assessments in this work.

Using a simple linear trend approach [36], the gradient and its variance of the resulting regression of the hydrological series with respect to time is used to check the possible trends

in the rainfall series. Based on the Wald statistics, the significance of trend gradients is tested based on a normally distributed assumption (significant level is 5%). Hannaford and Marsh [36] used a similar linear regression approach to look at runoff trends in the UK. Figure 11 shows series plots and their trend lines for the average annual rainfall for which show a significant downward trend for both A2 and B2 scenarios for the period 1961-2099 with acute trend for A2 scenario and that indicate climate change did take place since the observed period data.

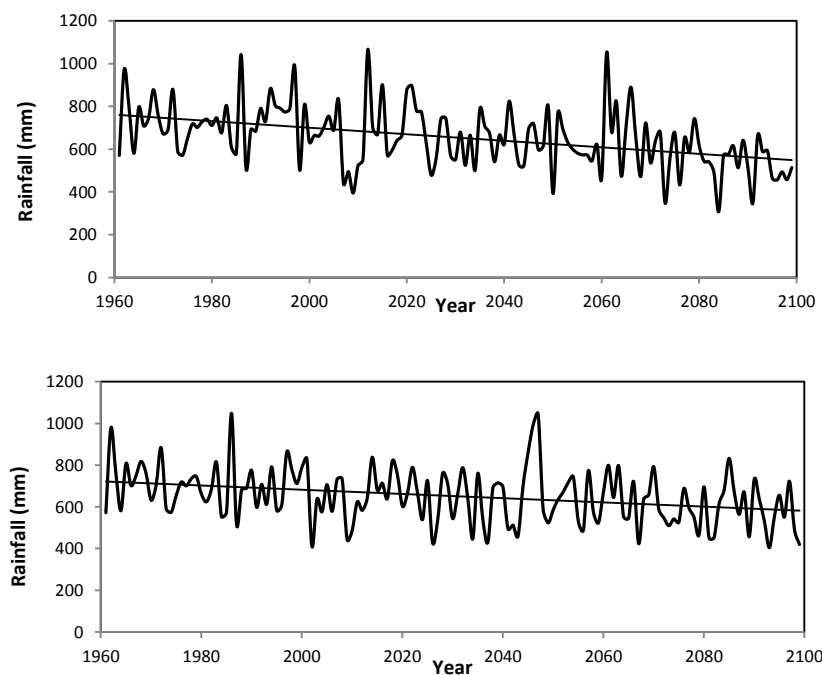


Fig. 11. Average annual rainfall for A2 scenario (upper) and B2 scenario (lower) compared with control period. Linear trend indicates that there is a significant downward trend

Figure 12 presents average monthly rainfall simulated by HadCM3 GCM for A2 and B2 scenarios of greenhouse emission for the three future periods compared with the baseline period. Both plots consistently project some reduction in the monthly rainfall for the 2020s, 2050s and 2080s; however 2080s experience largest drop especially during April and July months of A2 (51% and 77%) and during May and July of B2(49% and 79%) . Generally the projected rainfall in future varies significantly/slightly amongst the three future periods and the emission scenario considered as A2 experience more significant reduction than scenario B2.

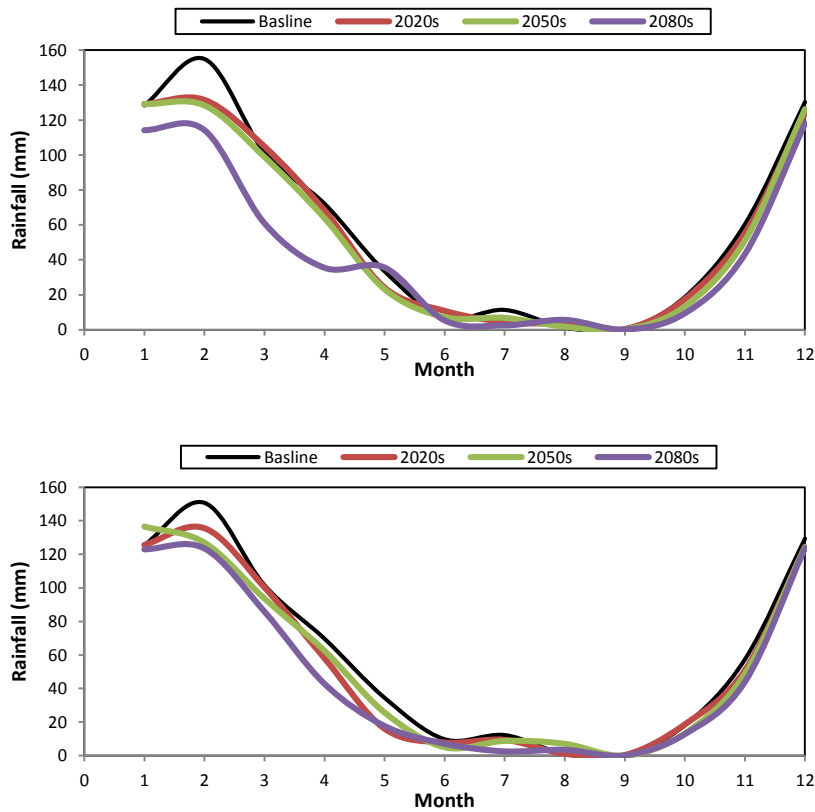


Fig. 12. Average monthly rainfall for A2 scenario (upper) and B2 scenario (lower) compared with baseline period

Other comparative plots of future periods against the baseline period is the daily rainfall box plots of the four seasons of A2 and B2 scenarios which were presented in Figure 13. The daily rainfall box plots are different across all seasons for the entire statistics with mix projections were found within the future periods. While the winter projects some increase/decrease in the daily rainfall statistics of wet days (maximum, 3rd quantile, mean, 1st quantile and minimum), the spring season show between very slight drop and no change for both scenarios. However both summer and autumn show a significant reduction in maximum rainfall value especially in 2080s while the other statistics remain nearly the same. In term of mean daily rainfall, a drop up to 8%, 6% and 24% for winter, spring and autumn respectively can be detected for A2 scenario by 2080s, while B2 projects a maximum drop of up to 6%, 10%, 48% and 18% for winter, spring, summer and autumn.

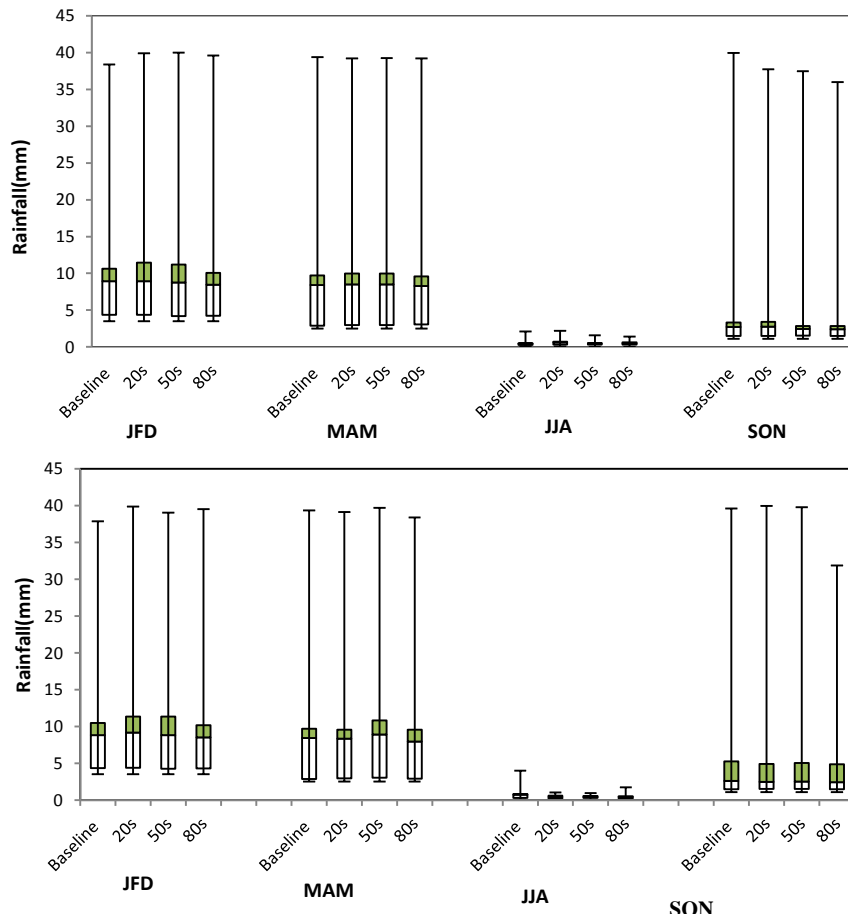


Fig. 13. The daily rainfall box plots across the four seasons for different future period of A2 scenario (upper) and B2 scenario (lower) compared with baseline period.

Moreover analysis for the obtained quantiles simulated by GEV revealed changes in the intensity and frequency (return period) of the extreme rainfall in the future periods of the 2020s, 2050s and 2080s for scenario A2 and B2 compared to the extreme rainfall derived from the observed baseline period 1961-1990 as in Figure 14. The extremes events are projected to decrease slightly in 2080s with highest decrease associated with A2 scenario. This because the rainfall under scenario A2 is more significant than under scenario B2 and temperature can be very hot and worse with increase in emission scenario which causes the moist air to be evaporated before going up and cause the rainfall. So the water vapour causing rainfall is reduced with increase the emission of greenhouse gas. The 2020s and 2050s showed no considerable change across the different return periods for A2 and B2 especially with the higher return period while the lower periods show some increase and decrease. The results obtained from the extreme analysis of rainfall in the future periods under climate change, clearly demonstrate that in general future extreme rainfalls are projected to be less frequent especially in 2080s with a very small drop are detected (up to 2%) due to location of

the study area. The return period of a certain rainfall will increase in the future as demonstrated by the dashed line for quantile-return period plot displayed in Figure 14 when a present storm of 20 year could occur once every 43 year in the 2080s. The results in Figure 14 also shows that an increase in the frequency of extreme rainfall depends on the return period, season of the year, the future period considered and the emission scenario under which it will occur.

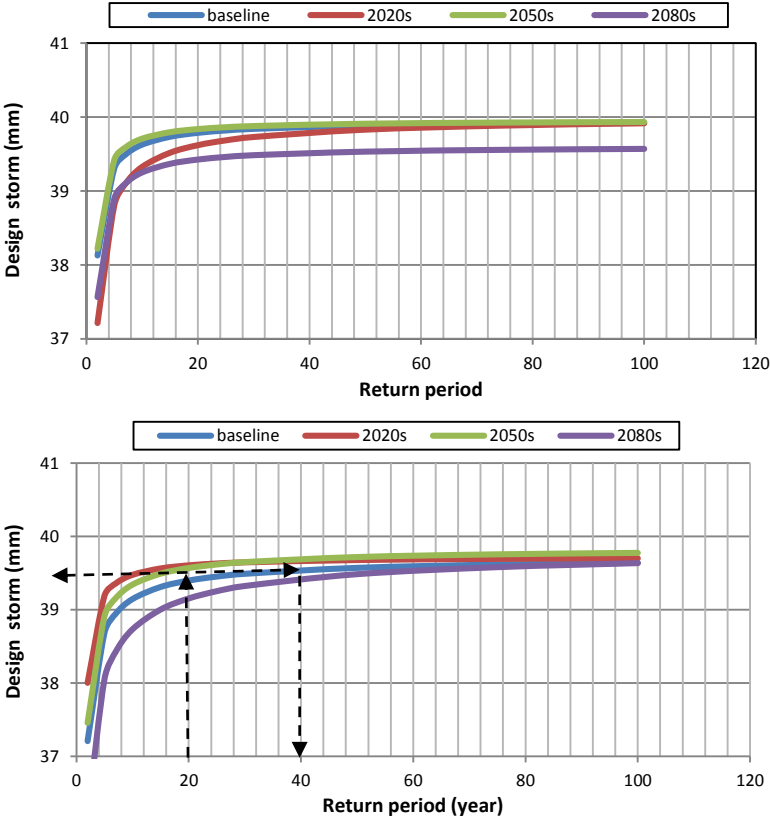


Figure 14. Future daily rainfall extremes for different return period of A2 scenario (upper) and B2 scenario (lower) compared with baseline period

6 Conclusions

Iraq is facing water shortage problems. One of the solutions to such problem is the use of water harvesting and artificial recharge of groundwater aquifers. These techniques greatly depend on rainfall events. In this research rainfall records were investigated in the northeast

part of Iraq to analyse the expected future rainfall trends. This will greatly help decision makers to set prudent water resources management plan.

Rainfall records of Sulaimani city dating back to 1961 were used in two scenarios A2 and B2. The medium high (A2) and medium low B2 scenarios have been used for purpose of this study as they are more likely than others scenarios, that beside the fact that no climate modelling center has performed GCM simulations for more than a few emissions scenarios (HadCM3 has only these two scenarios) otherwise pattern scaling can be used for generating different scenarios which entail a huge uncertainty. The outcome was averaged and divided by three (3) period of time, which are 2020s (2010-2039), 2050s (2040-2069) and 2080s (2070-2099) and compared with base line period (1961-1990). Climate change was assessed by comparing these three future time slices with baseline period of 1961-1990 as recommended by the Intergovernmental Panel of Climate change.

The results indicates that the average annual rainfall show a significant downward trend for both A2 and B2 scenarios for the period 1961-2099 with acute trend for A2 scenario and that indicate climate change did take place since the observed period data. Average monthly rainfall simulated by HadCM3 GCM for A2 and B2 scenarios of greenhouse emission for the three future periods compared with the baseline period show some reduction in the monthly rainfall for the 2020s, 2050s and 2080s; however 2080s experience largest drop especially during April and July months of A2 (51% and 77%) and during May and July of B2(49% and 79%) .

Generally the projected rainfall in future varies significantly/slightly amongst the three future periods and the emission scenario considered as A2 experience more significant reduction than scenario B2.

The daily rainfall box plots are different across all seasons for the entire statistics with mix projections were found within the future periods. While the winter projects some increase/decrease in the daily rainfall statistics of wet days (maximum, 3rd quantile, mean, 1st quantile and minimum), the spring season show between very slight drop and no change for both scenarios. However both summer and autumn show a significant reduction in maximum rainfall value especially in 2080s while the other statistics remain nearly the same.

In term of mean daily rainfall, a drop up to 8%, 6% and 24% for winter, spring and autumn respectively can be detected for A2 scenario by 2080s, while B2 projects a maximum drop of up to 6%, 10%, 48% and 18% for winter, spring, summer and autumn.

Moreover analysis for the obtained quantiles simulated by GEV revealed changes in the intensity and frequency (return period) of the extreme rainfall in the future periods for scenario A2 and B2 compared to the extreme rainfall derived from the observed baseline period. The extremes events are to decrease slightly in 2080s with highest decrease associated with A2 scenario. This because the rainfall under scenario A2 is more significant than under scenario B2 and temperature can be very hot and worse with increase in emission scenario which causes the moist air to be evaporated before going up and cause the rainfall. So the water vapour causing rainfall is reduced with increase the emission of greenhouse gas. The 2020s and 2050s showed no considerable change across the different return periods for A2 and B2 especially with the higher return period while the lower periods show some increase and decrease.

The return period of a certain rainfall will increase in the future when a present storm of 20 year could occur once every 43 year in the 2080s. The results also shows that an increase in the frequency of extreme rainfall depends on the return period, season of the year, the future period considered and the emission scenario under which it will occur.

Acknowledgments

The authors would like to thank Mrs. Semia Ben Ali Saadaoui of the UNESCO-Iraq for her encouragement and support. Thanks for Sulaimani University for providing some related data. The research presented has been financially supported by Luleå University of Technology, Sweden and by “Swedish Hydropower Centre-SVC” established by the Swedish Energy Agency, Elforsk and Svenska Kraftnät together with Luleå University of Technology, The Royal Institute of Technology, Chalmers University of Technology and Uppsala University. Their support is highly appreciated.

References

- [1] Al-Ansari, N. A.: Water resources in the Arab countries: Problems and possible solutions. UNESCO International conf. (Water: a looming crisis), Paris, 367-376, 1998.
- [2] Salem, F.: Water Sustainability-A National Security Issue for the Middle East and North Africa Region, 2nd International Water Conference in the Arab Countries; July 7-10, 2003.
- [3] Tolba, M. K.; El-Khouly O.A. and Thabet, K.A.: The Future of Environmental Action in the Arab World (in Arabic). UNEP/Environment Agency Abu Dhabi, 2001.
- [4] Kassas, M.: Aridity, Drought and Desertification, in Tolba, andf Saab, N., eds., Arab Environment and Future Challenges, Chapter 7, The Arab Forum For Environment and Development, 2008.
- [5] Naff, T.: Conflict and water use in the Middle East, in Roger, R. and Lydon, P. (Ed.), Water in the Arab Word: Perspectives and Prognoses, Harvard University, 253-284, 1993.

- [6] AL-Ansari, N. A.: Applied surface Hydrology, Al al-Bayt University publication, 2005.
- [7] Bazzaz, F.: Global climatic changes and its consequences for water availability in the Arab World, in Roger, R. and Lydon, P. (Ed.), Water in the Arab Word: Perspectives and Prognoses, Harvard University, 243- 252, 1993.
- [8] Voss K., Famiglietti, J., Lo, M., de Linage, C., Rodell, M. and Swenson, S.: Groundwater depletion in the Middle East from GRACE with implications for transboundary water management in the Tigris-Euphrates-Western Iran region, Water Resources Research, 49, 904-914, 2013.
- [9] Al-Ansari, N. A.: Management of Water Resources in Iraq: Perspectives and Prognoses, J. Engineering, 5, 667-684, 2013.
- [10] Elasha, B. O.: Mapping of Climate Change Threats and Human Development Impacts in the Arab Region, Uni- ted Nations Development programme, Arab Human Development Report (AHDR), Research Paper Series. 2010. <http://www.arab-hdr.org/publications/other/ahdrps/paper02-en.pdf>
- [11] IPCC (Intergovernmental Panel on Climate Change): Climate Change Impacts, Adaptation and Vulnerability, Cambridge University Press, Geneva, 2007.
- [12] Milly, P. C. D., Dunne, K. A and Vecchia, A. V.: Global Patterns of Trends in Streamflow and Water Availability in a Changing Climate,” Nature, Vol. 438, 347-350, 2005. doi:10.1038/nature04312
- [13] Al-Ansari, N. A. and Knutsson S.: Toward Prudent Management of Water Resources in Iraq, Journal of Advanced Science and Engineering Research, 1, 53-67, 2011.
- [14] United Nations: Water Resources Management White Paper, United Nations Assistance Mission for Iraq, United Nations Country Team in Iraq, 2010.
- [15] Al-Ansari, N. A., Salameh, E., and Al-Omari, I.: Analysis of Rainfall in the Badia Region, Jordan, Al al-Bayt University Research paper No.1, 66 p, 1999.
- [16] Al-Ansari, N. A., Al-Shamali, B., and Shatnawi, A.: Statistical analysis at three major meteorological stations in Jordan, Al Manara Journal for scientific studies and research 12, 93-120, 2006.
- [17] Al-Ansari, N. A. and Baban, S.: Rainfall Trends in the Badia Region of Jordan, Surveying and Land Information Science, 65, No 4, 233-243, 2005.
- [18] Kalnay, E., Kanamitsu, M., Kistler, R., Collins, W., Deaven, D., Gandin, L., Iredell, M., Saha, S., White, G., Woollen, J., Zhu, Y., Leetmaa, A., Reynolds, B., Chelliah, M., Ebisuzaki, W., Higgins, W., Janowiak, J., Mo, K. C., Ropelewski, C., Wang, J., Jenne, R. and Joseph, D.: The NCEP/NCAR 40-Year Reanalysis Project. Bulletin of the American Meteorological Society, 77 (3), 437-471, 1996.
- [19] Willmott, C. J., Rowe, C.M and Philpot, W. D.: Small-scale Climate Map: A Sensitivity Analysis of Some Common Assumptions Associated with the Grid-Point Interpolation and Contouring, American Cartographer, 12, (2), 5-16, 1985.
- [20] Shannon, D. A. and Hewitson, B. C.: Cross-scale Relationships Regarding Local Temperature Inversions at Cape Town and Global Climate Change Implications. South African Journal of Science, 92, (4), 213-216, 1996.
- [21] Crane, R. G. and Hewitson, B. C.: Doubled CO2 Precipitation Changes for the Susquehanna Basin: Down-Scaling from the Genesis General Circulation Model International Journal of Climatology, 18, 1, 65-76, 1998.
- [22] Giorgi, F. and Mearns, L.O.: Approaches to the simulation of regional climate change. Rev. Geophys, 29, 191-216, 1991.

- [23] Wilby, T. M. L., Wigley, D., Conway, P. D., Jones, B.C., Hewitson, J. M. and Wilks, D. S.: Statistical downscaling of general circulation model output: A comparison of methods, *Water Resources Research*, 34 (1998), 2995–3008, 1998.
- [24] Harpham, C., Wilby, R. L.: Multisite-Downscaling of heavy daily precipitation occurrence and amounts. *J. Hydrol*, 312, 1-21, 2005.
- [25] Abdellatif, M., Atherton, W., Alkhaddar, R.: Climate Change Impacts on the Extreme Rainfall for Selected Sites in North Western England, *Open Journal of Modern Hydrology*, 2(3), 49-58, 2012.
- [26] Hoai, N. D., Udo, K. and Mano, A.: Downscaling Global Weather Forecast Outputs Using ANN for Flood Prediction. *Journal of Applied Mathematics*, Article ID246286, 14 pages, 2011 doi:10.1155/2011/246286
- [27] CCIS (Canadian Climate Impacts Scenarios Group), 2010. Available online at: http://www.cics.uvic.ca/scenarios/index.cgi?More_Info-SDSM_Background
- [28] Levenberg, K.: A method for the solution of certain problems in least squares, *Quarterly of Applied Mathematics*, 5, 164–168, 1944.
- [29] Marquardt, D.: An algorithm for least-squares estimation of nonlinear parameters, *SIAM Journal on Applied Mathematics*, 11(2), 431–441, 1963.
- [30] Trigo, R.M.: Improving Meteorological Downscaling Methods with Artificial Neural Network Models. PhD thesis, University of East Anglia, 2000.
- [31] Nash, J. E., and Sutcliffe, J. V.: River flow forecasting through conceptual models, Part I - A discussion of principles, *J. Hydrol.*, 10, 282–290, 1970.
- [32] Schaap, M. G., and Leij, F. J.: Database related accuracy and uncertainty of pedotransfer functions. *Soil Science*, 16, 765-779, 1998.
- [33] Gupta, H.V, Sorooshian, S., Yapo, P.O.: Status of automatic calibration for hydrologic models: Comparison with multilevel expert calibration. *J Hydrologic Eng* 4, 135-143, 1999.
- [34] Coles, S.: An introduction to statistical modelling of extreme values. Springer Series in Statistic, London, 2001.
- [35] Jenkins, G., Perry, M., and Prior, G.: The Climate of the United Kingdom and recent Trends, Met Office Hadley Centre, Revised edition, ISBN 978-1-906360-05-4, 2009.
- [36] Hannaford, J., Marsh, T.: An assessment of trends in UK runoff and low flows using a network of undisturbed basins. *International Journal of Climatology*. 26(9), 1237–1253, 2006.